Chinese Journal of
POLYMER SCIENCE

RESEARCH ARTICLE

https://doi.org/10.1007/s10118-021-2649-1
Chinese J. Polym. Sci. **2022**, *40*, 175–184

Preheat Compression Molding for Polyetherketoneketone: Effect of Molecular Mobility

Xiao-Hua Zhang[a*], Meng-Xiao Jiao[a], Xin Wang[a], Bo-Lan Li[a], Feng Zhang[a], Yan-Bo Li[a], Jing-Na Zhao[b], He-Hua Jin[b], and Yu Yang[c]

[a] *Key Laboratory of Textile Science & Technology (Ministry of Education), College of Textiles, and Innovation Center for Textile Science and Technology, Donghua University, Shanghai 201620, China*
[b] *Advanced Materials Division, Suzhou Institute of Nano-Tech and Nano-Bionics, Chinese Academy of Sciences, Suzhou 215123, China*
[c] *Key Laboratory of Carbon Materials, National Engineering Laboratory for Carbon Fiber Technology, Institute of Coal Chemistry, Chinese Academy of Sciences, Taiyuan 030001, China*

Abstract Polyetherketoneketone (PEKK) is a new evolving polymeric material, and is considered as another important member of the polyaryletherketone (PAEK) family in addition to polyetheretherketone (PEEK). Hot compression molding can be used to compact and consolidate the PEKK products, where the temperature and pressure play key roles to affect the molecular mobility, entanglement and crystallization, and thus the mechanical properties of PEKKs. In this study, a preheating treatment was introduced in the compression molding, and it is found that such preheating is very essential to avoid the formation of crystal Form II, based on the increased chain entanglement. Molecular dynamics simulations revealed that the molecular mobility is always suppressed when a compression is applied. Therefore, by increasing the entanglement *via* the preheating and maintaining such entanglement in the consequent compression molding, strong and tough PEKK materials were obtained, with a negligible fraction of crystal Form II.

Keywords Polyetherketoneketone; Molecular mobility; Compression molding; Mechanical properties

Citation: Zhang, X. H.; Jiao, M. X.; Wang, X.; Li, B. L.; Zhang, F.; Li, Y. B.; Zhao, J. N.; Jin, H. H.; Yang, Y. Preheat compression molding for polyetherketoneketone: effect of molecular mobility. *Chinese J. Polym. Sci.* **2022**, *40*, 175–184.

INTRODUCTION

Polymer matrix composites are composed of a matrix from thermoset or thermoplastic and embedded glass, carbon, steel, or Kevlar fibers. Owing to their attractive combination of stiffness, toughness, light weight, corrosion resistance and so forth, such composites have been increasingly used in aerospace, marine, automotive, sports equipment, and many other engineering fields. Toward next generation high-performance thermoplastic composites, poly-aryl-ether-ketones (PAEKs), a family of semi-crystalline thermoplastics, have shown superior advantages of better mechanical properties and higher temperature applications.[1] Among the various PAEKs, poly-ether-ether-ketone (PEEK) and poly-ether-ketone-ketone (PEKK) are the most widely used candidates.[2–6] PEKK matrix has similar mechanical properties (slightly stiffer and stronger) but a lower melting temperature than PEEK, resulting in a wider process window, and thus is becoming more and more attractive. Different from PEEK, which is mainly synthesized by a nucleophilic substitution route, PEKK is often prepared by Friedel-Crafts acylation reaction.[7–9] Based on the ratio between terephthaloyl chloride (T) and isophthaloyl chloride (I) in the precursor (the third compound is diphenyl ether), PEKK molecules are named according to the T/I ratio, such as PEKK 60/40, 70/30, and 80/20. Specially, the I content connects benzene rings *via* the *meta*-position, and thus causes a curled molecular segment. Consequently it is easier for PEKK to get entangled with its neighbors.

In the composite manufacturing process for thermoplastics, heating and compression are the fundamental treatments for stock shapes, such as plates or thick sheets.[1,10] For both PEEK and PEKK, it has been investigated and shown that the thermal history can strongly affect the crystallization behavior and thus the physical properties.[11–23] For instance, Lustiger *et al.*[13] investigated various molding and aging conditions for PEEK-based carbon fiber composites, and found that the slow cooling and annealing conditions lead to a much higher crystallinity for PEEK; Conrad *et al.*[16] showed that an increased molding temperature can lead to increased compressive modulus, yield strength and yield strain, for compression molded hydroxyapatite/PEEK composites; Mylläri *et al.*[17] observed the reduced thermal stability of PEEK during a long time aging at high temperatures (*e.g.*, above 250 °C); and Wang *et al.*[22] demonstrated that a pre-stretching at temperatures above the glass transition temperature (T_g) can be an effective way to improve the mechanical pro-

* Corresponding author, E-mail: zhangxh@dhu.edu.cn
Received August 12, 2021; Accepted September 29, 2021; Published online November 20, 2021

perty of PEEK. Thus far, there have been quite sufficient investigations on the microstructure, crystallization behavior, and mechanical properties for PEEK and its composites, while a deep exploration on PEKK is not sufficient. However, it is still of great necessity as PEKK is quite different from PEEK in the molecular structure, polarity, crystalline structure, dissolubility, and processability.

Very recently, there have been several important investigations on PEKK. For instance, Benedetti *et al.*[24] developed a new procedure to correlate the crystallinity and mechanical performance with the process conditions for laser sintered PEKK. Tencé-Girault *et al.*[25] revealed the effect of cold crystallization on amorphous PEKK (T/I=60/40) by using a series of quantitative analysis, *e.g.*, small-angle X-ray scattering (SAXS), wide-angle X-ray scattering (WAXS), and differential scanning calorimetry (DSC) data. Li *et al.*[26] used molecular dynamics (MD) to characterize an extensive set of properties of PEKK, including the lattice parameters and stability of the crystal structures, glass transition and melting temperatures, crystal/amorphous interfacial energy, and enthalpy of fusion. Thus far, for the most widely used compression molding, there is no clear processing profile for PEKK, which should be quite different from those for PEEK and other thermoplastics due to the different molecular structures. Specially, to the best of our knowledge, preheating has been often considered, while the pressure is always applied during the whole process of the current compression molding. This might cause problems to PEKK, as its molecular mobility is suppressed by its high molecular polarity.

Herein, we report that a preheating at a low pressure is a necessary stage to improve the mechanical properties of PEKK. Experimentally, the preheating was found to induce a higher entanglement of PEKK chains, leading to the prevention of the formation of crystal Form II. By using molecular dynamics simulations, the mobility was quantitatively reflected by the time-dependence variation of atomic displacement, which is dependent on the pressure applied on the system. Therefore, to better control the crystallinity and thus the mechanical properties of PEKK, great attention should be paid to the pretreatment before the compression molding, and other manufacturing processes such as injection molding and 3D printing.

METHODS

Compression Molding

Semicrystalline PEKK was synthesized with terephthaloyl chloride, isophthaloyl chloride, and diphenyl ether, under a T/I ratio of 60/40. The compression molding was used to prepare the PEKK specimens (90 mm × 10 mm × (0.8–1.0) mm), with an HG-3622M Electrical Forming Machine (Heng Guang Science & Technology Co., Ltd., Kunshan, China). Fig. 1(A) shows the schematics of different processing stages, where a preheating treatment was applied before the molding, different from the conventional treatment where the compression is usually triggered in the beginning.[23] Therefore, by also considering the compression and heating sequences during the annealing stage, there are 2 × 2 strategies for the whole molding process, see Fig. 1(B). For the conversion from the initial state to the molded state, *i.e.*, the melted state under compression, the pressure can be applied either before or after the heating-up, as referred by +P+T and +T+P. Similarly, the annealing can be either –P–T or –T–P. Thus the 2 × 2 types of processing can be TPPT, TPTP, PTPT and PTTP, with Fig. 1(C) showing four typical processing profiles. Note that all the PEKK samples were prepared directly from the powder form, to avoid the effect of melt memory or thermal history.

Here, the pressure was the value applied on the PEKK samples, about 50 MPa, by dividing the load with the sample's area (90 mm × 10 mm). The temperature for the preheating was always the same as the molding temperature (T_{mold}), and was set to 340, 360, 380, and 400 °C in this study. The holding time for the preheating and molding was about 1 h and >40 min, respectively, and the annealing time was >45 min. It was found that by extending the time for any procedure, there was no distinguishable results for the physical properties of the final PEKK sheets.

Characterization

The DSC characterization was performed with a DSC analyzer (HS-DSC-101, Shanghai HESON Instrument Technology Co., Ltd., Shanghai, China) in N_2 atmosphere. The heating rate was 10 °C/min. The bi-Gaussian fitting was used to fit DSC curves for the evaluation of the position and melting enthalpy for different endotherm peaks. The DSC crystallinity was calculated by

$$\chi_c = \frac{\Delta H_m}{\Delta H_{100\%}} \times 100\% \quad (1)$$

where ΔH_m indicates the melting enthalpy and $\Delta H_{100\%}$ is the melting enthalpy of the 100% crystalline polymer matrix, usually taken as 130 J/g.[21,27] The X-ray differaction (XRD) characterization was performed with a Bruker D8 Advance XRD (Karlsruhe, Germany) using Cu Kα radiation (λ = 1.54 Å). The tensile properties were obtained by using an Instron 5967 Universal Testing Machine (UTM) (Instron Corp., Norwood, USA), with a gauge length ranging from 1 cm to 2 cm and a tensile rate of 1 mm/min. The DMA analysis was performed with a Q800 Dynamic Mechanical Thermal Analysis (TA Instruments, New Castle, USA) in the tensile mode at a heating rate of 5 °C/min and a temperature range of 30–270 °C. The dimension of samples was 40 mm long, 10 mm wide, and about 1 mm thick.

MD Simulation

In order to understand how the PEKK chain mobility affects the molding procedure and crystallization behavior, all-atom MD simulations were conducted for PEKK polymers with a T/I ratio of 60/40. The simulation was performed on 12 identical PEKK chains, having a chemical form of

$$C_6H_5-[O-C_6H_4-CO-C_6H_4-CO-C_6H_4]_{46}-O-C_6H_5 \quad (2)$$

or $[EKK]_{46}E$ in abbreviation. The link between the neighboring ketones was randomly set to be *para*- or *meta*-positioned, with a 60 to 40 probability by using a random number. The OPLS-AA force field[28] was used to assign the atom types for PEKK, including the OPLS_145 and OPLS_146 for the C and H atoms in benzene ring, OPLS_177 for the O atom in ether, and OPLS_280 and OPLS_281 for the C and O atoms in ketone. The simulations were conducted by using the MD package GROMACS (versions 2018.1 and 2021).[29,30] The integration time step is 1 fs. The initial configuration was obtained by placing the 12 PEKK chains at positions as far away from each other, and then under a series

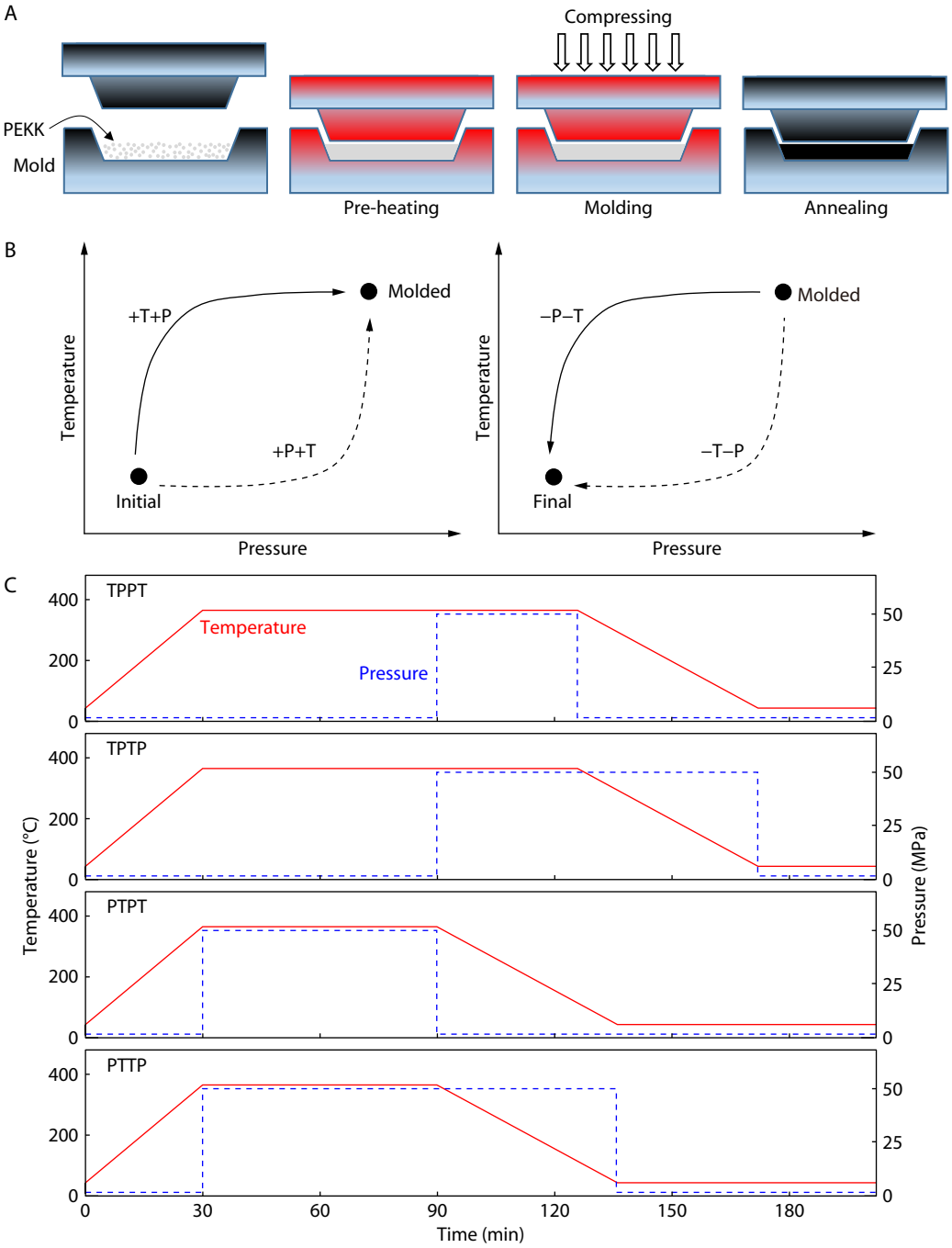

Fig. 1 Revised processes for compression molding. (A) Schematics for the different processing stages; (B) Different procedures from the initial to the molded state, and from the molded to the final state. The plus and minus symbols correspond to the increasing and decreasing, respectively; (C) Four different pressure and temperature profiles during compression molding process for PEKK.

of NVT simulation with decreasing volume of the simulation box, these chains got to a condensed state. After then, simulations were performed in NPT (constant number of particles, pressure, and temperature) ensemble where the temperature T and pressure P were controlled by using the Berendsen algorithm.[31] The time constant was $\tau_T = \tau_P = 10$ ps for both the thermostat and pressure coupling. The compressibility was set to $\beta = 5\times10^{-4}$ bar^{-1}. Such combination of τ_P and β were found to be available for thermoplastics, which are much more compressible than water.

The molding profiles shown in Fig. 1(C), namely the TPPT, TPTP, PTPT, and PTTP, were considered in the MD simulations, where T was gradually increased from 350 K to 700 K, and P was set to 5 and 100 bar, respectively. At each group of T and P, the simulation was conducted for at least 20 ns. The chain mobility was evaluated by calculating the mean square dis-

https://doi.org/10.1007/s10118-021-2649-1

placement (MSD) of one PEKK molecule by

$$\mathrm{MSD} = \frac{1}{N}\sum_{i=1}^{N} |\vec{r}_i(t) - \vec{r}_i(0)|^2 \quad (3)$$

from a much longer simulation over 120 ns, where N is the total atom number of the PEKK molecule and $\Delta\vec{r}_i = \vec{r}_i(t) - \vec{r}_i(0)$ is the displacement of atom i. Its slope against time in the first tens of ns was taken as the diffusion or reptation ability, and when the stabilized state is reached, the mean square displacement no longer grows up but fluctuates with time.

RESULTS AND DISCUSSION

Tensile Properties

Fig. 2(A) shows four typical stress-strain curves for different PEKK sheets. The conventional treatments without using the preheating, *i.e.*, PTPT and PTTP, resulted in a brittle feature, where the strain at break was just up to 2.3%. On the contrary, the preheated TPPT and TPTP samples were not brittle, and thus the tensile strength (for the TPTP sample, the ultimate strength)

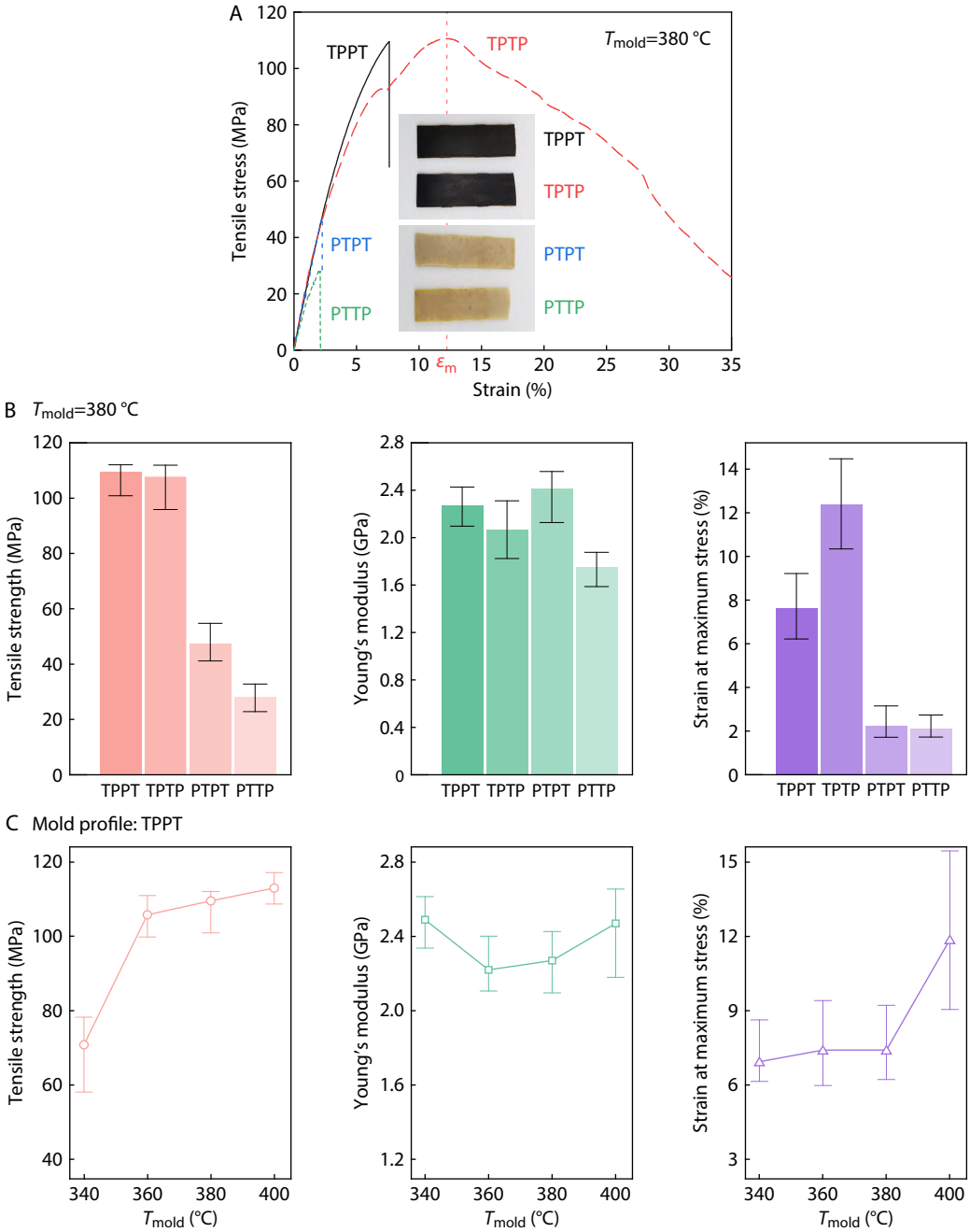

Fig. 2 Mechanical properties of PEKK sheets. (A) Typical stress-strain curves for the four molding treatments. For the TPTP sample, ε_m indicates the strain at the maximum tensile stress, which is identical to the strain at break for the other samples; (B) Comparisons in tensile strength, Young's modulus, and strain at maximum stress for the four PEKK samples obtained at T_{mold}=380 °C; (C) The strength, modulus, and strain at maximum stress (ε_m) as functions of T_{mold} for the TPPT processing.

https://doi.org/10.1007/s10118-021-2649-1

could exceed 108 MPa, higher than that of the sample without being preheated. Specially, the TPTP sample did not break after reaching the maximum stress (the ultimate strength), indicating that a necking deformation occurred. In other words, the TPTP showed a certain ductility, corresponding to an improved capacity to absorb mechanical overload.[32] Clearly, as shown in Fig. 2(B), the preheating treatments (TPPT and TPTP) ensured a high tensile strength and toughness, while the samples without being preheated (PTPT and PTTP) were quite brittle. Nevertheless, the difference in modulus is not large, owing to the intrinsic rigidness of PEKK molecular chain.

Generally, the molding temperature is the first-rank parameter in compression molding, following by the pressure-holding time, compression pressure, cooling rate, mold-opening temperature, and so on.[33] Therefore, it is necessary to know how T_{mold} affect the mechanical properties. Fig. 2(C) shows the strength, modulus, and strain at break (identical to ε_m) of the TPPT samples obtained at different T_{mold}. At the low T_{mold}=340 °C, although the melting has been activated, the temperature is not enough to induce a high mobility of the molecular chain segments. As a result, the initial polymer entanglement cannot be efficiently (or fully) optimized, leading to a certain high rigidness. Thus, such sample exhibited the highest modulus (2.49 GPa) and the smallest strength (70.8 MPa) and strain at break (6.9%). When T_{mold} is above 360 °C, the molecular mobility is increased to allow a sufficient relaxation of the entangled molecular chains. Overall, the strength, modulus, and strain at break all gradually grow up with increasing T_{mold} from 360 °C to 400 °C. Interestingly, the 400 °C-molded sample showed the largest strain at break, up to 11.9%, also showing a bit ductility (similar to the TPTP sample).

Fig. 3 compares the fracture morphologies between the TPPT specimens and one TPTP-380 specimen, where the number indicate the value of T_{mold}. The TPPT-400 and TPTP-380 specimens all exhibited a ductile fracture, different from the brittle fracture for the others. For these plastic specimens, the plastic deformation was quite evident, and there was also a clear necking phenomenon. Such different fracture morphologies can be ascribed to the different entanglements of polymer chains.[34] Obviously, the preheating treatment and high molding temperature can induce a high mobility of PEKK chains and thus an enhanced entanglement, and the compressed cooling (the case of TPTP) can well maintain such entanglement.

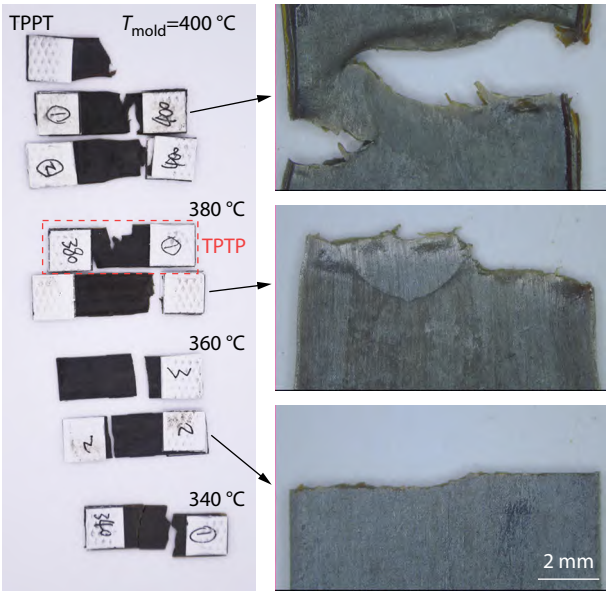

Fig. 3 Fracture morphologies of PEKK specimens. The TPTP-380 and TPPT-400 samples exhibited larger strains at break as compared to the others.

Crystallinity

PEKK exhibits a multiple melting behavior with increasing the temperature, corresponding to a polymorphism and multiple endothermic peaks.[35,36] Fig. 4(A) compares the DSC curves between PEKK samples, where the main difference is at the melting regions. To simply the comparison process, the four types of samples are provided just for T_{mold}=380 °C, while for the other temperatures just the TPPT and PTPT are provided. Generally, all the non-preheated samples (PTXX) exhibited a small endothermic peak for the glass transition, around 167 °C. Above the glass transition, there were a small peak called the lower temperature endotherm (LTE), and a large peak called the higher temperature endotherm (HTE), which can even be divided into two or more endothermic peaks. The LTE peak gradually weakened and up-shifted to higher temperature (from 235 °C to 265 °C) with increasing T_{mold} from 340 °C to 400 °C. Differently, there is no clear variation in the HTE peak. All the PTXX samples showed a mixed HTE peak containing two sub-peaks (HTE_1 and HTE_2) at around 305 and 330 °C, which are related to the crystal Form II and Form I, respectively. Based on these DSC curves, the melting enthalpy (ΔH_m^{HTE}) and crystallinity (χ_c^{HTE}) for the HTE peaks were obtained, see Table 1. (The enthalpy and crystallinity were divided into two constituents if there were two sub-peaks.) For the four PTPT examples, the crystallinities both reached maximum at 380 °C, and then decreased at 400 °C. When the molding profile was changed to PTTP, *i.e.*, a different cooling procedure, the overall variation in crystallinity was the same, just with slightly smaller values. Clearly, the PTPT-380 was the optimal profile.

Unfortunately, although the crystallinity was quite high for the PTPT-380 specimen, the tensile property was still very limited (Fig. 2A). Clearly the crystallinity might not be the primary factor to affect the mechanical property. We speculate that the coexistence of crystal Form I and Form II can induce nonuniformity in PEKK, and the amorphous phase connecting these crystals might become fragile with the growing-up of the crystals. Furthermore, it is known that cold crystallization of PEKK leads to the coexistence of Form I and Form II while melt crystallization yields to mostly Form I.[35,37] Here, after the molding, the melt PEKK underwent a cooling process from T_{mold} to room temperature, it was indeed a melt crystallization, but with a result containing two crystal forms. This should be due to the lack of a preheating treatment.

Therefore, as a comparison, the PEKKs were molded by using the TPXX profiles, and the crystallinities were quite different. The only exception is the TPPT at 340 °C, where two HTE sub-peaks can still be observed. For the other TPXX samples there is just one HTE peak locating at an in-between temperature of 315–318 °C (Table 1). This significant change well in-

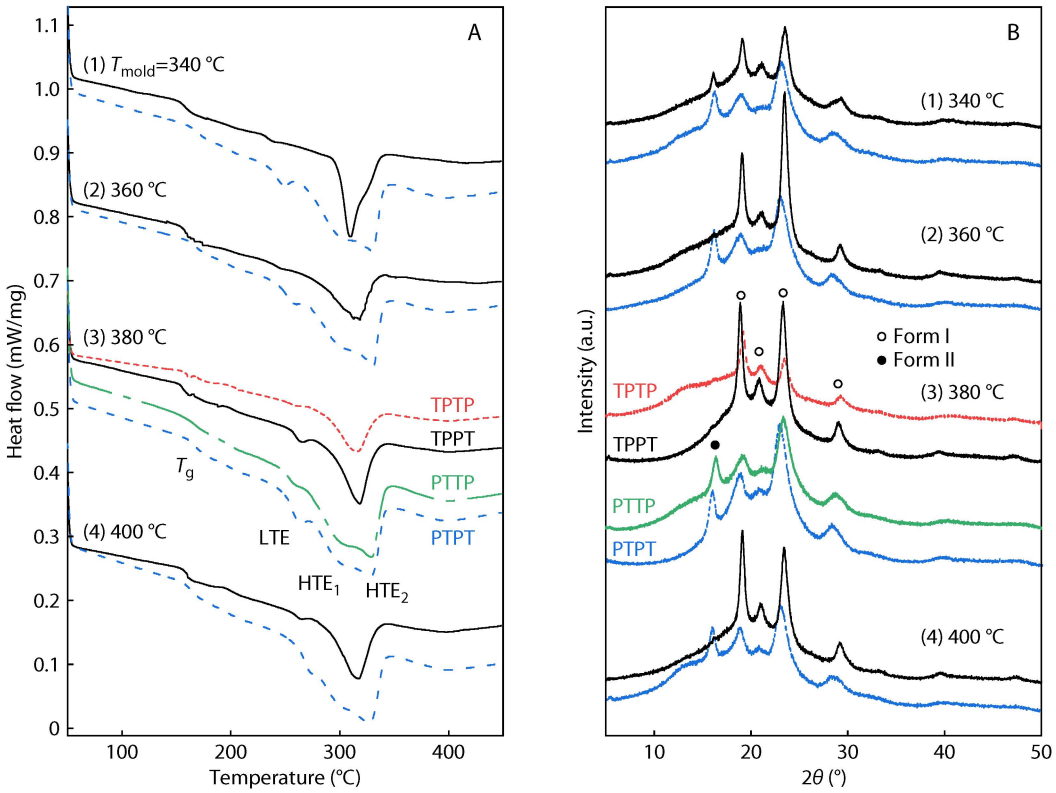

Fig. 4 Crystallinity characterization by using the DSC thermograms (A) and XRD diffractograms (B). A full comparison is provided for T_{mold} = 380 °C, while for other molding temperatures only the PTPT and TPPT are plotted.

dicated the effect of preheating. When T_{mold} is not high (e.g., 340 °C), the PEKK chains cannot possess a high molecular mobility to induce a strong crystallization of Form I, but a mobility sufficient for Form II. This is because the Form I has a higher crystal surface free energy than the Form II, and thus a slower nucleation rate.[35] On the contrary, at a higher T_{mold} without compression, the PEKK chains get a higher mobility, making it possible to form the edge-to-face phenyl packing by suppressing the face-to-face packing, as the latter is energetically less stable. Otherwise, if the compression is applied, the mobility would be suppressed to induce the crystallization of Form II. As a result, the crystallinity of Form I in the preheated TPXX PEKKs was higher than that in the PTXX PEKKs. For example, it was 20.6% and 13.4% for the TPPT-380 and PT-PT-380 specimens.

Table 1 T_g, T_{LTE}, T_{HTE}, ΔH_m^{HTE}, and χ_c^{HTE} of the PEKK samples shown in Fig. 4, according to the DSC characterization. There are two quantities if the HTE contains two sub-peaks.

Method	T_{mold} (°C)	T_g (°C)	T_{LTE} (°C)	T_{HTE} (°C)	ΔH_m^{HTE} (J/g)	χ_c^{HTE} (%)
PTPT	340	171	248	305, 330	23.89, 13.98	18.4, 10.8
	360	168	259	305, 330	26.13, 15.80	20.1, 12.2
	380	167	265	305, 327	26.57, 17.45	20.4, 13.4
	400	164	275	305, 327	20.01, 15.74	15.4, 12.1
PTTP	380	168	261	304, 328	21.52, 17.81	16.6, 13.7
TPPT	340	158	238	309, 325	23.48, 8.34	18.1, 6.4
	360	160	246	318	26.67	20.5
	380	158	255	318	26.72	20.6
	400	160	265	317	25.07	19.3
TPTP	380	160	261	315	23.96	18.4

The different crystallinities were also characterized by XRD, as shown in Fig. 4(B). The preheated TPXX samples exhibit XRD peaks at diffraction angles 2θ=19.1°, 21.1°, 23.4°, and 29.2°, associated to the diffraction of the (110), (111), (200), and (211) crystalline planes of Form I, respectively. The (110) and (200) peaks are the strongest, indicating that the crystallization took place mainly along these two planes. For the unpreheated PTXX samples, the (110) peak is much weaker than the (200) peak. This means that the preheating can improve the crystallization along the (110) plane. Furthermore, there is an additional (020) peak of Form II at 2θ=16.1°, in agreement with the DSC characterization. Clearly, there is a competition between the chain mobility and the crystallization of Form II. The higher chain mobility, the less fraction of Form II. This provides a fundamental philosophy to control the fractions of crystal Form I and Form II. Here, the preheating TPXX treatments can guarantee a high chain mobility and thus induce the solo crystallization of Form I.

Mass Density

The above PEKK samples showed different mass densities due to the different crystallinities. The PTXX (360–400 °C) samples had a higher mass density of 1.290–1.318 g/cm^3, with a certain large variation, and the TPXX (360–400 °C) were slightly lighter but more constant, of 1.275–1.294 g/cm^3. Such difference agrees well with the crystallinity calculated in Table 1, indicating that the crystallization induces the more densified packing of PEKK molecules. By considering the higher mechanical properties as discussed above, it becomes

https://doi.org/10.1007/s10118-021-2649-1

interesting that *the lighter, the stronger*.

Hence, it is suspected that the mechanical properties are more determined by the adhesion or connection between the crystallized phase and amorphous phase, rather than the individual components. For the PTXX samples, the crystal content is high, leading to a high rigidness, while the amorphous content is less, causing the less efficient load transfer between the crystals. Therefore, these samples were brittle and not strong. On the contrary, the amorphous state dominates and well connects the crystals in the TPXX samples, resulting in an uniform load transfer within the sample, and a high toughness as well.

Dynamic Mechanical Analysis

The different crystallinity of PEKK can also affect the viscoelastic properties. The storage modulus (E'), loss modulus (E''), and loss tangent (tanδ) between the TPPT-380 and PTPT-380 specimens are compared in Fig. 5, by using the dynamic mechanical analysis (DMA). The PTPT-380 specimen exhibited a much higher E'', but a similar E'. The larger loss modulus of the PTPT specimen can be ascribed to the high crystallization of Form II (see Fig. 4 and Table 1). As the crystallization is a shrinkage process, the connection between the crystallized phase and amorphous phase is even more loose than both of them. As a result, such crystal/amorphous connection is weak in mechanical properties, especially under dynamic loadings. Therefore, on one hand, the PTPT samples were brittle, as already shown in Fig. 2, and on the other hand, the crystals were easy to move under vibrational loading, corresponding to the higher damping ability.

Besides the DSC thermograms, the peak of loss tangent in DMA is also used to determine the glass transition temperature (the DMA T_g), which is usually slightly higher than the DSC T_g. Fig. 5 shows that the DMA T_g was about 161 and 179 °C.

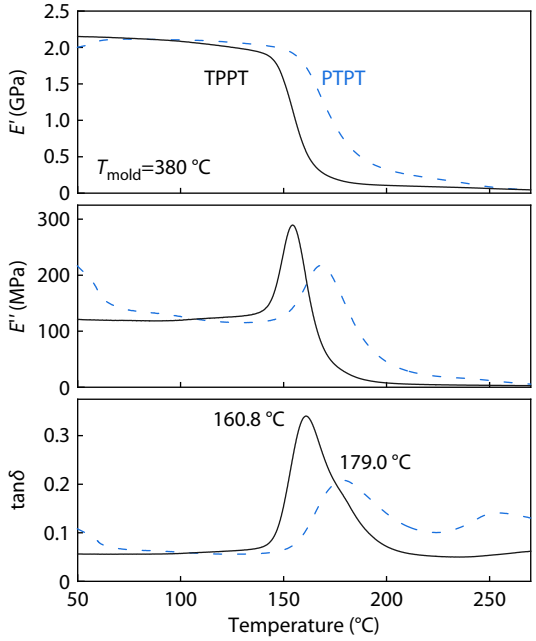

Fig. 5 Dynamic mechanical properties (E', E'', and tanδ) of the TPPT-380 and PTPT-380 PEKK specimens.

Such difference is in agreement with the DSC characterization. Clearly, although the TPXX treatments increased the crystallinity of Form I, the overall crystallinity was remarkably suppressed due to the limited crystallization of Form II. As the crystals can conduct heat more efficiently, thus the more crystallized PTXX samples can not only void heat accumulation at the crystal/amorphous contacts, but also absorb the heat more quickly than the amorphous state. Therefore, the glass transition can be postponed to higher temperatures. This is confirmed by performing the DSC characterizations at a higher heat rate of 15 °C/min, which resulted in T_gs of 160 and 175 °C for the TPPT-380 and PTPT-380 samples, respectively. Clearly, the glass transition of PTPT sample was shifted more to higher temperatures according to Table 1, as a result of the larger amount of crystals.

MOLECULAR DYNAMICS SIMULATION

In order to explore how the PEKK chain mobility affects the molding procedure and crystallization behavior, all-atom MD simulations were conducted for PEKK polymers with a T/I ratio of 60/40. Due to the presence of *para*- and *meta*-positioned ketone links (Fig. 6A), the PEKK chain can easily fold, twist, and/or rotate in the topological space. Therefore, the molded structure of PEKK strongly depends on the way of chain entanglement, and the processing history has an important influence.

To mimic the molding of PEKK powders, the 12 PEKK chains were initially placed far away from each other (*e.g.*, has a distance larger than 10 nm). First, the simulation box was artificially compressed to induce the van der Waals (vdW) interactions between these chains, and then the NPT ensemble was used to simulate the molding procedure. Therefore, it can be possible to analyze the chain entanglement based on the atomic distribution of PEKK chain in the molded structure.

Effect of Preheating

Fig. 6(B) shows the direct compression with a small pressure of 5 bar at 350 K. It took a very long time (more than 100 ns) to reach a steady state. The final mass density was 1.185 g/cm^3. From the snapshot shown in Fig. 6(C), there are evident pores between PEKK chains (as labelled by the red ellipses), corresponding to the aggregation of PEKK particles rather than an efficient interpenetration between them. The pore size was even up to 1.6 nm along the longest dimension. The 12 PEKK molecules were all localized with a low degree of entanglement (interpenetration) with each other, as shown by one PEKK presented by using large-size spheres. This is because at low temperatures the PEKK chain has a very limited molecular mobility, and cannot deform its structure to reduce the system energy. Therefore, it is necessary to increase the temperature above the melting temperature.

Then a TPTP procedure was simulated in this study, as shown in Fig. 6(D). First, the heating was performed at a low pressure of 5 bar, up to 700 K, identical to a preheating treatment. Thus the PEKK chains could go into a melt state, and interpenetrate with each other as much as possible. The mass density first grew up to 1.202 g/cm^3 at T=400–410 K, indicating that the pores were growing smaller. When T became further higher, the mass density gradually decreased as a result

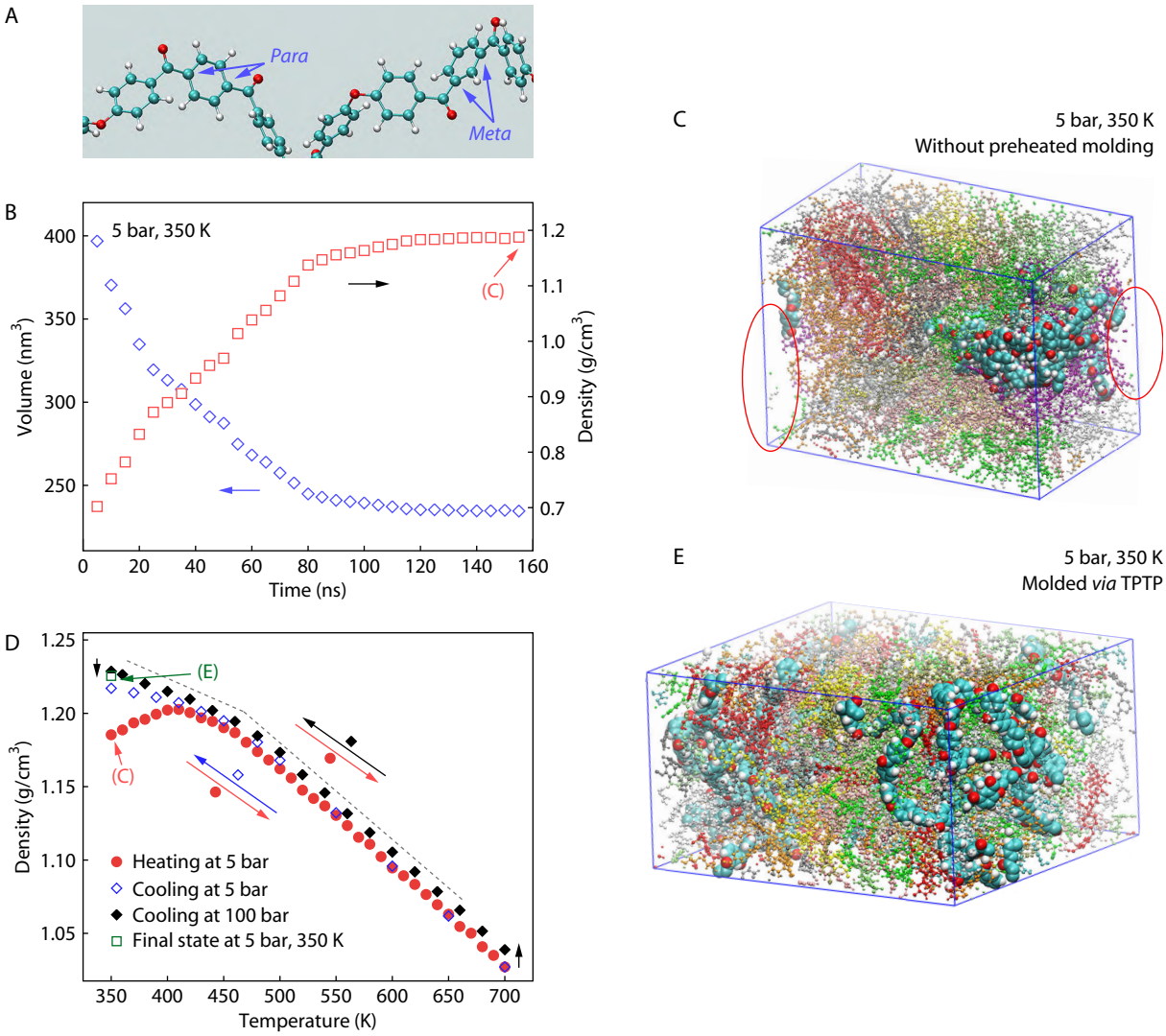

Fig. 6 MD simulation of a TPTP procedure. (A) A PEKK segment containing the *para*- and *meta*-positioned ketone links; (B) The direct compression at 350 K and a low pressure of 5 bar; (C) A snapshot of the final structure of (B). Each PEKK molecule is plotted by using a different color, and for one molecule the atoms are plotted by large-size spheres, with the cyan, white, and red colors refer to C, H, and O atoms, respectively. A large-size pore is marked by red ellipses; (D) A TPTP procedure, as labelled by the red and black arrows. The initial and final structures are shown in (C) and (E), respectively; (E) There were no evident pores TPTP-treated PEKKs, and the molecular entanglement (interpenetration) became much stronger.

of thermal expansion. Then, the hot PEKKs were compressed to 100 bar, to suppress the mobility. Consequently, the PEKKs were cooled down to 350 K, and then released to 5 bar. Such process is obviously a TPTP treatment, and is labelled by using the red and black arrows in Fig. 6(D). In the final structure (Fig. 6E), no clear pores can be observed and the PEKK represented by large spheres can be seen to distribute in a much larger space, corresponding to a high degree of entanglement (interpenetration) with other PEKKs. Therefore, the final PEKKs had a mass density of 1.224 g/cm^3. (Note that before the pressure release, the mass density was 1.229 g/cm^3.)

If the cooling was realized at the low pressure of 5 bar, see the blue empty diamonds in Fig. 6(D), the final structure had a mass density of 1.216 g/cm^3. First, the preheating had already induced a high degree of entanglement, which was well maintained by the two different cooling processes. However, as the low pressure still ensured a certain high mobility during the cooling process, the entanglement at high temperature could change by the further motion of PEKK chains. This causes the slight expansion in the simulation, and should be an important factor concerning with the crystallization of Form II.

Suppressed Mobility

If the heating is performed under high pressures, identical to the PTXX treatments, the molecular mobility is still weak even at high temperatures. Such situation could be a severe problem during the 3D printing by the high melt viscosity.[38] In order to reveal the effect of pressure on the molecular mobility, the stabilized simulations were further conducted for tens of ns, from which the mean square displacement was evaluated. Fig. 7 compares the MSD for the 700 K simulations at 5 and 100 bar, respectively. The two MSD curves both grew up with time in the

https://doi.org/10.1007/s10118-021-2649-1

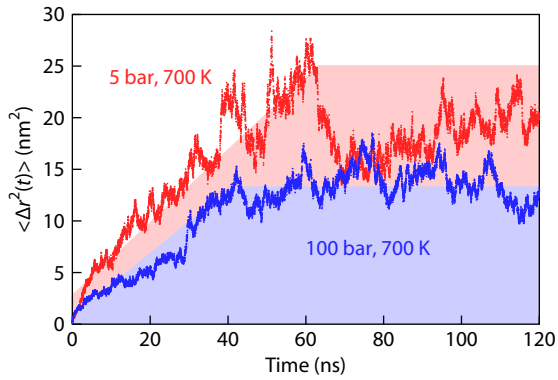

Fig. 7 Mean square displacement of one PEKK molecule during long-time MD simulations. The molecule can diffuse or reptate more when a smaller pressure is applied. After a sufficiently long time, the curves no longer grow up, corresponding to the attenuation of the diffusion.

first tens of ns. The low pressure simulation showed a higher growing rate of 0.44 nm^2/ns, about 76% larger than the other one of 0.25 nm^2/ns. This is quite like a diffusion behavior, concerning with the reptation in entangled polymers. However, after a sufficiently long time, such diffusion attenuated as reflected by the fluctuation in MSD.

Clearly, when the pressure is increased, the polymer mobility is suppressed, and the diffusion or reptation would stop within a short period of time. (The fluctuation plateau onset at about 40 and 65 ns for the simulations, see the in Fig. 6D.) Therefore, it becomes difficult to reach a high entanglement for the polymer chains. This provides a molecular explanation of the effect of mobility that plays a key role in the chain entanglement, and thus an understanding of the necessity of the preheating treatment. However, different from the simulation on the crystallization of PEKK based on a united-atom description,[26] the present simulation did not show evident crystallization processes possibly due to the lack of description on initial nucleation. (This is also a possible reason for the smaller mass density as compared to the experimental measurement.) Therefore, in future investigations, more attention should be paid to the problem that how the different crystal forms can be affected by the chain entanglements.

Note that the molecular length in MD is much shorter than that in the real PEKK. Thus the remarkable difference in MSD at different pressures also indicates a dependence of molecular weight on the mobility, because the shorter the length, the higher the mobility. This can also be reflected experimentally by the increased rate of solvent-induced crystallization for the PEKK with ultrasonication-reduced molecular weights (to be reported elsewhere). Reminiscently, an M^{-2} dependence has been reported for the rate of crystallization of PEEK.[39]

CONCLUSIONS

PEKK chains can highly entangle with each other by introducing a preheating treatment before the compression molding, as the direct compression can strongly limit the molecular mobility even at temperatures above the melting one. By using the preheat compression molding, the crystal Form II can be remarkably suppressed, and the crystallinity of Form I can be enhanced. As the same cooling processes were used, such crystallinity difference was ascribed to the different entanglements in PEKK melts. This study points out a correct strategy to compact and consolidate PEKK products, which can also be applied in injection molding and 3D printing.

NOTES

The authors declare no competing financial interest.

ACKNOWLEDGMENTS

This work was financially supported by the Fundamental Research Funds for the Central Universities (No. 2232021G-01) and the National Natural Science Foundation of China (No. 51862036).

REFERENCES

1 Al-Mezrakchi, R.; Creasy, T.; Sue, H. J.; Bremner, T. Manipulation of thick-walled PEEK bushing crystallinity and modulus *via* instrumented compression molding. *J. Appl. Polym. Sci.* **2021**, *138*, 49930.
2 Alqurashi, H.; Khurshid, Z.; Syed, A. U. Y.; Rashid Habib, S.; Rokaya, D.; Zafar, M. S. Polyetherketoneketone (PEKK): an emerging biomaterial for oral implants and dental prostheses. *J. Adv. Res.* **2021**, *28*, 87–95.
3 Attwood, T. E.; Dawson, P. C.; Freeman, J. L.; Hoy, L. R. J.; Rose, J. B.; Staniland, P. A. Synthesis and properties of polyaryletherketones. *Polymer* **1981**, *22*, 1096–1103.
4 Audoit, J.; Rivière, L.; Dandurand, J.; Lonjon, A.; Dantras, E.; Lacabanne, C. Thermal, mechanical and dielectric behaviour of poly(aryl ether ketone) with low melting temperature. *J. Therm. Anal. Calorim.* **2019**, *135*, 2147–2157.
5 Benedetti, L.; Brulé, B.; Decraemer, N.; Davies, R.; Evans, K. E.; Ghita, O. A route to improving elongation of high-temperature laser sintered PEKK. *Addit. Manuf.* **2020**, *36*, 101540.
6 Berendsen, H. J. C.; Postma, J. P. M.; van Gunsteren, W. F.; DiNola, A.; Haak, J. R. Molecular dynamics with coupling to an external bath. *J. Chem. Phys.* **1984**, *81*, 3684–3690.
7 Blundell, D. J.; Osborn, B. N. The morphology of poly(aryl-ether-ether-ketone). *Polymer* **1983**, *24*, 953–958.
8 Cebe, P.; Chung, S. Y.; Hong, S. D. Effect of thermal history on mechanical properties of polyetheretherketone below the glass transition temperature. *J. Appl. Polym. Sci.* **1987**, *33*, 487–503.
9 Cheng, S. Z. D.; Ho, R. M.; Hsiao, B. S.; Gardner, K. H. Polymorphism and crystal structure identification in poly(aryl ether ketone ketone)s. *Macromol. Chem. Phys.* **1996**, *197*, 185–213.
10 Choupin, T.; Debertrand, L.; Fayolle, B.; Régnier, G.; Paris, C.; Cinquin, J.; Brulé, B. Influence of thermal history on the mechanical properties of poly(ether ketone ketone) copolymers. *Polym. Cryst.* **2019**, *2*, e10086.
11 Conrad, T. L.; Jaekel, D. J.; Kurtz, S. M.; Roeder, R. K. Effects of the mold temperature on the mechanical properties and crystallinity of hydroxyapatite whisker-reinforced polyetheretherketone scaffolds. *J. Biomed. Mater. Res. Part B* **2013**, *101B*, 576–583.
12 Dar, U. A.; Xu, Y. J.; Zakir, S. M.; Saeed, M. U. The effect of injection molding process parameters on mechanical and fracture behavior of polycarbonate polymer. *J. Appl. Polym. Sci.* **2017**, *134*, 44474.

13 Day, M.; Deslandes, Y.; Roovers, J.; Suprunchuk, T. Effect of molecular weight on the crystallization behaviour of poly(aryl ether ether ketone): a differential scanning calorimetry study. *Polymer* **1991**, *32*, 1258–1266.
14 Gardner, K. H.; Hsiao, B. S.; Faron, K. L. Polymorphism in poly(aryl ether ketone)s. *Polymer* **1994**, *35*, 2290–2295.
15 Hess, B.; Kutzner, C.; van der Spoel, D.; Lindahl, E. GROMACS 4: algorithms for highly efficient, load-balanced, and scalable molecular simulation. *J. Chem. Theory Comput.* **2008**, *4*, 435–447.
16 Jiang, Z.; Chen, R.; Lu, Y.; Whiteside, B.; Coates, P.; Wu, Z.; Men, Y. Crystallization temperature dependence of cavitation and plastic flow in the tensile deformation of poly(ε-caprolactone). *J. Phys. Chem. B* **2017**, *121*, 6673–6684.
17 Jones, D. P.; Leach, D. C.; Moore, D. R. Mechanical properties of poly(ether-ether-ketone) for engineering applications. *Polymer* **1985**, *26*(9), 1385–1393.
18 Jorgensen, W. L.; Maxwell, D. S.; Tirado-Rives, J. Development and testing of the opls all-atom force field on conformational energetics and properties of organic liquids. *J. Am. Chem. Soc.* **1996**, *118*, 11225–11236.
19 Kumar, D.; Rajmohan, T.; Venkatachalapathi, S. Wear behavior of PEEK matrix composites: a review. *Mater. Today: Proc.* **2018**, *5*, 14583–14589.
20 Kurtz, S. M.; N. Devine, J. PEEK biomaterials in trauma, orthopedic, and spinal implants. *Biomaterials* **2007**, *28*, 4845–4869.
21 Lee, Y.; Porter, R. S. Effects of thermal history on crystallization of poly(ether ether ketone) (PEEK). *Macromolecules* **1988**, *21*, 2770–2776.
22 Li, C.; Strachan, A. Prediction of PEKK properties related to crystallization by molecular dynamics simulations with a united-atom model. *Polymer* **2019**, *174*, 25–32.
23 Lustiger, A.; Uralil, F. S.; Newaz, G. M. Processing and structural optimization of PEEK composites. *Polym. Compos.* **1990**, *11*, 65–75.
24 Men, Y. Critical strains determine the tensile deformation mechanism in semicrystalline polymers. *Macromolecules* **2020**, *53*, 9155–9157.
25 Mullins, M. J.; Woo, E. P. The synthesis and properties of poly(aromatic ketones). *J. Macromol. Sci. Rev. Macromol. Chem. Phys.* **1987**, *C27*, 313–341.
26 Mylläri, V.; Ruoko, T. P.; Vuorinen, J.; Lemmetyinen, H. Characterization of thermally aged polyetheretherketone fibres —mechanical, thermal, rheological and chemical property changes. *Polym. Degrad. Stab.* **2015**, *120*, 419–426.
27 Roland, S.; Moghaddam, M.; Tencé-Girault, S.; Fayolle, B. Evolution of mechanical properties of aged poly(ether ketone ketone) explained by a microstructural approach. *Polym. Degrad. Stab.* **2021**, *183*, 109412.
28 Rudolph, N. M.; Osswald, T. A.; Ehrenstein, G. W. Influence of pressure on volume, temperature and crystallization of thermoplastics during polymer processing. *Int. Polym. Proc.* **2011**, *26*, 239–248.
29 Sarasua, J. R.; Remiro, P. M.; Pouyet, J. Effects of thermal history on mechanical behavior of PEEK and its short-fiber composites. *Polym. Compos.* **1996**, *17*, 468–477.
30 Seguela, R. Critical review of the molecular topology of semicrystalline polymers: the origin and assessment of intercrystalline tie molecules and chain entanglements. *J. Polym. Sci. Part B: Polym. Phys.* **2005**, *43*, 1729–1748.
31 Shukla, D.; Negi, Y. S.; Uppadhyaya, J. S.; Kumar, V. Synthesis and modification of poly(ether ether ketone) and their properties: a review. *Polym. Rev.* **2012**, *52*, 189–228.
32 van der Spoel, D.; Lindahl, E.; Hess, B.; Groenhof, G.; Mark, A. E.; Berendsen, H. J. C. GROMACS: fast, flexible, and free. *J. Comput. Chem.* **2005**, *26*, 1701–1718.
33 Tencé-Girault, S.; Quibel, J.; Cherri, A.; Roland, S.; Fayolle, B.; Bizet, S.; Iliopoulos, I. Quantitative structural study of cold-crystallized PEKK. *ACS Appl. Polym. Mater.* **2021**, *3*, 1795–1808.
34 Veazey, D.; Hsu, T.; Gomez, E. D. Next generation high-performance carbon fiber thermoplastic composites based on polyaryletherketones. *J. Appl. Polym. Sci.* **2017**, *134*, 44441.
35 Wang, P.; Yu, H.; Ma, R.; Wang, Y.; Liu, C.; Shen, C. Temperature-dependent orientation of poly(ether ether ketone) under uniaxial tensile and its correlation with mechanical properties. *J. Therm. Anal. Calorim.* **2020**, *141*, 1361–1369.
36 Wang, Q.; Xue, Q.; Liu, H.; Shen, W.; Xu, J. The effect of particle size of nanometer ZrO_2 on the tribological behaviour of PEEK. *Wear* **1996**, *198*, 216–219.
37 Xie, J.; Wang, S.; Cui, Z.; Wu, J. Process optimization for compression molding of carbon fiber-reinforced thermosetting polymer. *Materials* **2019**, *12*, 2430.
38 Xu, Q.; Shang, Y.; Jiang, Z.; Wang, Z.; Zhou, C.; Liu, X.; Yan, Q.; Li, X.; Zhang, H. Effect of molecular weight on mechanical properties and microstructure of 3D printed poly(ether ether ketone). *Polym. Int.* **2021**, *70*, 1065–1072.
39 Zhang, X. Carbon nanotube/polyetheretherketone nanocomposites: mechanical, thermal, and electrical properties. *J. Compos. Mater.* **2021**, *55*, 2115–2132.

https://doi.org/10.1007/s10118-021-2649-1